Novel Chewing Cycle Approach for Peak Detection Algorithm of Chew Count Estimation

Nur Asmiza Selamat, *Member, IEEE*, Sawal Hamid Md Ali, *Senior Member, IEEE*, Ahmad Ghadafi Ismail, *Member, IEEE*, Siti Anom Ahmad, *Senior Member, IEEE*, and Khairun Nisa' Minhad, *Member, IEEE*

***Abstract*—Chew count is a critical parameter in analyzing mastication signals, yet traditional methods of manual counting by trained clinicians are often labor-intensive and prone to errors. As a result, there has been a growing interest among researchers in developing automated methods for estimating chew count. This article reviews the existing approaches, evaluates their effectiveness, and proposes a new approach based on optimization technique. This work proposes a novel approach to chew count estimation using particle swarm optimization (PSO) combined with a peak detection algorithm. The chewing dataset comprises signals collected from 20 participants consuming eight different food types, with proximity sensors (PSs) detecting temporalis muscle activity. The peak detection algorithm identifies key signal features, while PSO optimizes the peak prominence and width parameters to minimize the mean absolute error (MAE) in chew count estimation. Two specific chewing cycle approaches were implemented: a participants-based (P) cycle and a participants-food type-based (PF) cycle. These approaches were compared to the traditional All (A) chewing cycle method, which evaluates chew count across the entire dataset in a single analysis. Results demonstrate that the PF method yields the lowest MAE at 1.25%, followed by the P method at 3.46%, and the A method at 4.26%. Moreover, the PF method required the least computational time at 8012.2 s, compared to 9392.0 s for the P method and 36 621.4 s for the A.**

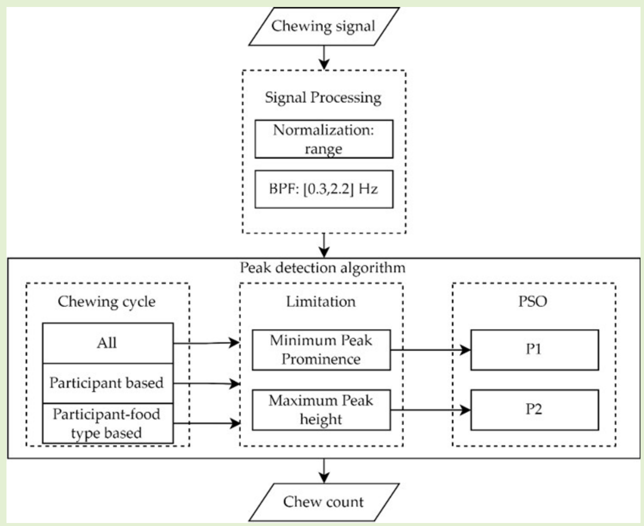

***Index Terms*—Chew count estimation, chewing cycle, chewing episode, maximum peak width, minimum peak prominence, particle swarm optimization (PSO), peak detection.**

I. Introduction

MONITORING food intake involves assessing nutritional information that reflects an individual's eating habits, including the timing, duration, and frequency of eating episodes [1]. This information is crucial for understanding dietary patterns that contribute to obesity [2]. The use of sensors to detect hand-to-mouth actions, biting, chewing, and swallowing has significantly advanced food intake monitoring, especially in the past year [1], [3]. Chewing is a critical activity that provides detailed nutritional information, as it is directly involved in the food intake process, from biting to swallowing.

For food intake monitoring applications, chewing data can be used to understand individual eating patterns and habits [4]. Three key questions arise when studying eating behavior: 1) Is the user eating? 2) What is the user eating? and 3) How much is the user eating? [5]. The data collected can be classified into dietary intake (i.e., what and how much is consumed), eating behaviors (i.e., food choices, motives, habits, and events), and

Received 21 August 2024; revised 9 October 2024; accepted 18 October 2024. Date of publication 13 November 2024; date of current version 2 January 2025. This research funded by Universiti Teknikal Malaysia Melaka and and Universiti Kebangsaan Malaysia (under Grant No. DIP-2023-008). The authors also acknowledge support from International Centre for Theoretical Physics, ICTP through the Associates Programme (2022–2027). Finally, the authors wish to express their gratitude to the Ministry of Education Malaysia for the funding support. The associate editor coordinating the review of this article and approving it for publication was Prof. Runhuai Yang. *(Corresponding author: Nur Asmiza Selamat.)*

Please see the Acknowledgment section of this article for the author affiliations.

Digital Object Identifier 10.1109/JSEN.2024.3487150

context (i.e., who is eating, when, where, with whom, etc.) [6]. To gain a comprehensive understanding of dietary habits, it is essential to track the dynamic process of eating episodes, often referred to as meal microstructure.

Meal microstructure encompasses various aspects of food intake behavior, including total eating episode duration (from the start of food intake to the end, including pauses), true ingestion duration (time spent chewing), number of eating events (a bite followed by chewing and swallowing), ingestion rate, chewing frequency and efficiency, and bite size [4]. Studies have shown a clear relationship between food intake rate and energy intake, suggesting that examining meal microstructure could offer new insights into obesity [7].

Mastication, commonly known as chewing, is the process of breaking down food using teeth. Sensor-based systems can automatically detect and analyze chewing, extracting data, such as the number of chews, chewing speed (frequency), chewing time, chewing force (strength), cycle duration, and skull vibration [8]. This information can classify food types and estimate food volume, representing stages 2 and 3 in automatic food intake monitoring [9] (with stage 1 being the detection of food intake). For instance, Wang et al. [8] utilized dynamic mastication parameters to identify food types based on different food properties. Chewing and swallowing counts are also used to estimate energy intake [10]. Yang et al. [4] combined chewing duration and chew count with bite and swallow features to estimate mass and energy intake, Hussain et al. [11] focused on using chewing and swallowing cycles to identify food types, volume, and calorie count.

Among the various mastication dynamics, chew count is the most commonly used parameter for advancing food intake monitoring. Chew count is one of the mastication parameters extracted and analyzed from the chewing signal. Manually counting chews by trained clinicians and the effort involved in studies enlisting even small number of subjects is large considering the number of chews per minute. The process is tedious, time-consuming, and error prone. Several researchers have focused on estimating chew count. In the literature, several approaches of manual and automatic chew counts estimation have been proposed.

Farooq and Sazonov [12] developed a peak detection algorithm based on chewing signal peaks to estimate chew count, employing both semi-automatic and fully automatic approaches [13]. They later used linear regression methods to estimate chew count by extracting features, such as the number of peaks, valleys, zero crossings, and the duration of chewing sequences [14], [15]. Hossain et al. [7] used video-based methods to count chews by extracting the number of peaks, while Alshboul and Fraiwan [16] also employed video data for chew counting based on peak detection from processed signals.

According to the literature, most chew counting methods rely on peak counting or a combination of other characteristics of chewing signals. For instance, some studies have extracted the number of peaks, chewing sequence duration, and zero crossings [15], while others have included the number of valleys [14]. Hossain et al. [7] and Farooq and Sazonov [12] used the numbers of peaks and the number of peak-to-peak [17] without implementing restrictions. Several researchers implemented the peak detection algorithm limitation to reduce the mean absolute error (MAE) (improving the chew count). For example, some studies introduced threshold values to count peaks exceeding a certain value [13], while others implemented limitations on peak height or used peak prominence [18] and width to refine peak detection [16].

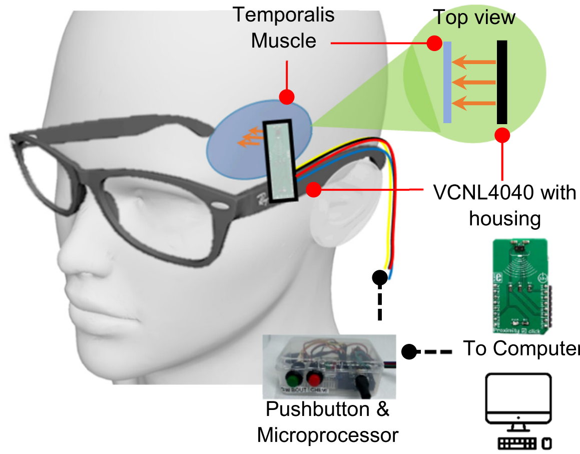

Fig. 1. Chewing detection system.

In chewing count estimation, the previous study used and extracted the features of number of peaks [12], [13], [14], [15], valleys [14], zero crossings [14], [15], and the duration [14], [15]. The performances of MAE of the previously proposed approach were 3.43% (laboratory) [15], 5.42% $\pm$ 4.61 (slow) [16], 8.09% $\pm$ 7.16% [12], 9.66% [14], 10.4% $\pm$ 7.0% (semi-automatic) [13], 11.1% (calculated) [7], 12.2% [19], and 15.0% $\pm$ 11.0% (automatic) [13].

A new approach to chew counting, based on a particle swarm optimization (PSO)-based peak detection algorithm, has been proposed, achieving an MAE of 4.26% [20]. This algorithm counts peaks that meet specific criteria for prominence and width, with the parameters optimized using PSO to minimize MAE. However, the approach is prone to accumulating errors due to the need to balance overall performance, potentially missing or incorrectly detecting some peaks.

The main contributions of this article are as follows.

1) Introducing two new approaches to improve the PSO-based peak detection algorithm: one based on chewing cycle participants and the other on participant-food types.
2) Analyzing and comparing these new approaches with the existing PSO-based algorithm, evaluating MAE, total chew count, percentage difference in MAE, and time consumption.
3) Comparing the literature that utilizes peak detection approaches for chew counting estimation.

II. Chewing Detection System

In this study, we utilized the chewing detection system proposed by Selamat and Ali [21], as illustrated in Fig. 1.

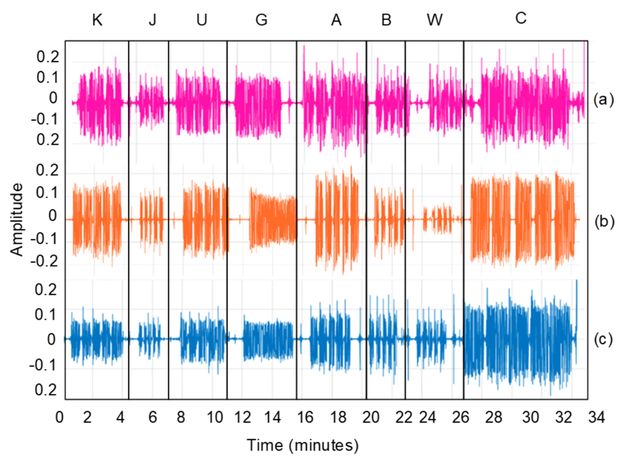

Fig. 2. Example of the preprocessed chewing signal of three participants. (a) Participant 3, (b) Participant 9, and (c) Participant 13.

The system was developed using a wearable eyeglass device equipped with a proximity sensor (PS), an Arduino Nano, and two pushbuttons. The sensor was programmed to detect signals from the temporalis muscle movement, which were combined with signals from the pushbuttons. The data were read by a computer using Microsoft Excel with the Data Streamer add-in, interfacing with the Arduino Nano board at a sampling rate of 50 Hz. Further data processing was conducted on the computer, with data validation based on the labeling of chewing episodes.

The study involved 20 participants, all of whom were thoroughly briefed and provided informed consent. Data collection occurred in a controlled environment, focusing on both eating and resting activities. For the eating portion, eight types of food were served in controlled portions per spoonful and per size. Apple (A), banana (B), watermelon (W), and carrot (C) were served in spoonful portions, while crackers, jelly, gummy candy, and chewing gum were served in standardized sizes.

For classification and chew count estimation, MATLAB 2022a (MathWorks, Inc.) was utilized. The raw data were preprocessed using normalization and filtering methods. Initially, the "range" normalization method was applied to eliminate amplitude variations caused by different participants. A low-pass filter, with a cutoff frequency range of 0.3–2.2 Hz, was then implemented to remove dc components and retain the signal relevant to chewing. According to Selamat et al. [20], this system achieved a mean accuracy of 96.37% across 20 participants, with the highest accuracy recorded at 98.48%.

The preprocessed chewing signals for three participants are shown in Fig. 2, highlighting the amplitude variations due to differences in participants and food types.

III. Chew Count Estimation

Chew count is a key mastication parameter extracted and analyzed from chewing signals. In previous studies, chew count estimation has been achieved by combining features, such as the number of peaks, the duration of the chew sequence, and the number of zero crossings. The characteristics of these extracted features used for counting chews are illustrated in Fig. 3. An abstract diagram provides an overview of the proposed chew count estimation method.

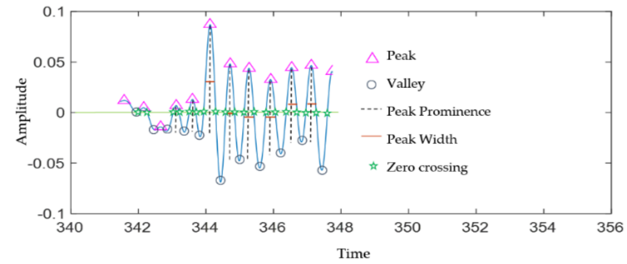

Fig. 3. Features extracted for chew count estimation.

A. Peak Detection Algorithm

The peak detection algorithm is designed to identify the preferred chewing cycle and the start and end times of all related chewing episodes for each preprocessed chewing signal. The algorithm then extracts peaks from the chewing signal, focusing on their prominence and width characteristics. These features are critical for eliminating insignificant peaks caused by nonchewing activities. The prominence of the peaks reflects the opening and closing of the jaw (temporalis muscle), while the width of the peaks corresponds to chewing frequency [20].

The algorithm uses a minimum peak prominence and maximum peak width to filter out irrelevant peaks, ensuring that only significant chewing-related peaks are considered. Both parameters are essential for accurate chew count estimation, as they directly relate to jaw movement and chewing frequency [20]. To account for individual variations in chewing patterns—due to factors, such as food hardness [18], sensor placement, face shape, and jaw structure—the average peak prominence and width are calculated for each chewing episode.

To further refine the algorithm and reduce time consumption, a multiplier parameter is introduced, determined using PSO. This approach simplifies the process by optimizing the search parameters based on three defined chewing cycles. This article also presents new approaches that are participant-based and participant-food type-based, enhancing the method presented in previous studies [20].

B. Particle Swarm Optimization

PSO is one of the most effective metaheuristic optimization techniques, known for its simplicity and ease of implementation. By defining an appropriate objective function, PSO can achieve optimal results for chew count estimation. In this study, we adopted an inertia-weight (ω)-based PSO algorithm. The algorithm determines the multipliers for the average prominence and width of peaks using PSO. The objective function minimizes the sum of the absolute differences between the estimated and actual chew counts (labeling), as expressed in equation.

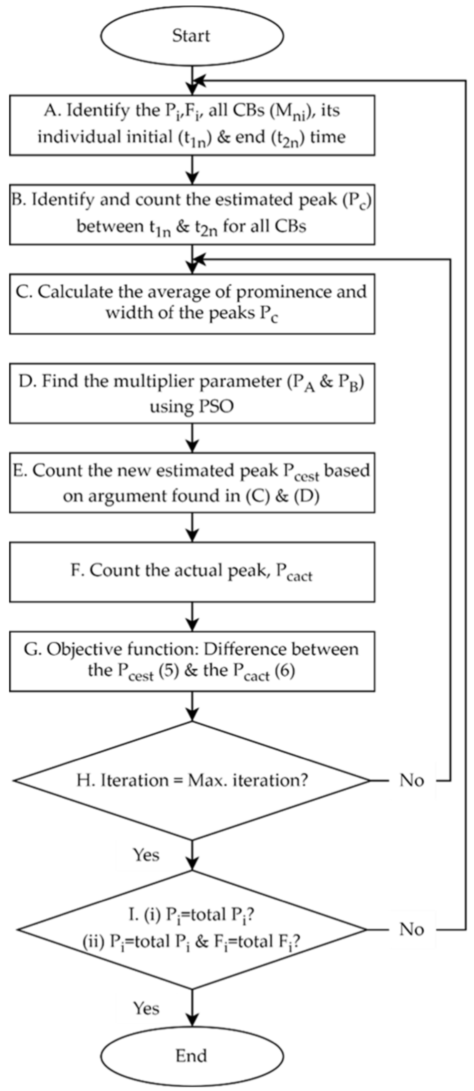

Fig. 4. PSO-peak detection algorithm.

Since the peak patterns of chewing can vary depending on participants and food types, PSO searches for the multipliers that best suit each chewing episode, resulting in the smallest possible overall error in chew count estimation, as shown in (2) and (3). Here, Min.pp represents the minimum peak prominence, Max.pw represents the maximum peak width, L is the total chew count, M is the respective chewing episode, and P_A and P_B are the parameters contributing to the optimized error.

The flow of developing the PSO-based peak detection algorithm is illustrated in Fig. 4, where P_i is the participant number, F_i is the food type sequence, M_{ni} corresponds to the chewing episode for the respective participant, and t_{1n} and t_{2n} are the start and end times of the respective chewing bout (n), P_c identifies the peak for the respective chewing bout, while P_A and P_B are the multipliers for the minimum peak prominence and maximum peak width, respectively, obtained using PSO. Finally, P_{cact} and P_{cest} represent the actual and estimated peak counts after applying the algorithm

$$|\text{Total Error}| = \sum_{m=1}^{M} \left| P_{C_{\text{Act}}}(n) - P_{C_{\text{Est}}}(n) \right| \quad (1)$$

$$\text{Min.pp (M)} = \left[\frac{1}{L} \sum_{l=1}^{L} \text{Peak prominence (M)} \right] \times P_A \quad (2)$$

$$\text{Max.pw (M)} = \left[\frac{1}{L} \sum_{l=1}^{L} \text{Peak width (M)} \right] \times P_B. \quad (3)$$

C. Chewing Cycle

Determining the window size is a crucial step in chew count estimation, as a larger window is required for estimating chew count than for chewing classification. The approach in [20] addresses variations in chewing patterns among participants by using the average prominence and width within each chewing episode. To simplify the process, PSO is employed to find a constant multiplier that optimizes chew count estimation. This article will implement, analyze, and compare three different chewing cycles (segmentation).

1) *Chewing Cycle Based on All Episodes:* This method determines the PSO parameter values based on a single chewing cycle for the entire dataset. The PSO algorithm searches for two parameter values—prominence and peak width multipliers—across all data. The stopping criterion for this method is the maximum number of iterations in the PSO.
2) *Participant-Based Chewing Episodes:* This method determines the PSO parameter values based on 20 chewing cycles, each corresponding to one participant. The PSO searches for two parameters (prominence and peak width multipliers) for each participant, resulting in a set of two parameters for each of the 20 chewing cycles. The stopping criterion is the maximum number of iterations per participant, continuing until all participants have been processed [as shown in Fig. 4, I.(i)].
3) *Participant-Food Type-Based Chewing Episodes:* This method determines the PSO parameter values based on 160 chewing cycles, derived from eight food types across 20 participants. The PSO searches for two parameters (prominence and peak width multipliers) for each chewing cycle, resulting in a set of two parameters for each of the 160 cycles. The stopping criterion is the maximum number of iterations per cycle, continuing until all participants and food types have been processed [as shown in Fig. 4, I.(ii)].

In this study, the term "chewing cycle" refers to the segmentation of data from the 20 participants to determine the PSO parameter values. The implementation of the chewing cycle to find the PSO parameters is illustrated in Fig. 5, where P represents the participants, and PF represents the participant-food type combinations. The numbering corresponds to the respective participant, and the color coding in PF indicates the food type.

D. Analysis of the Estimated Chew Count

The performance of chew count estimation for an individual participant is evaluated using the percentage of absolute error between the actual chew count (C_{Act}) and the estimated chew count (C_{Est}), as shown in (4). The overall system performance is assessed by calculating the MAE across all participants,

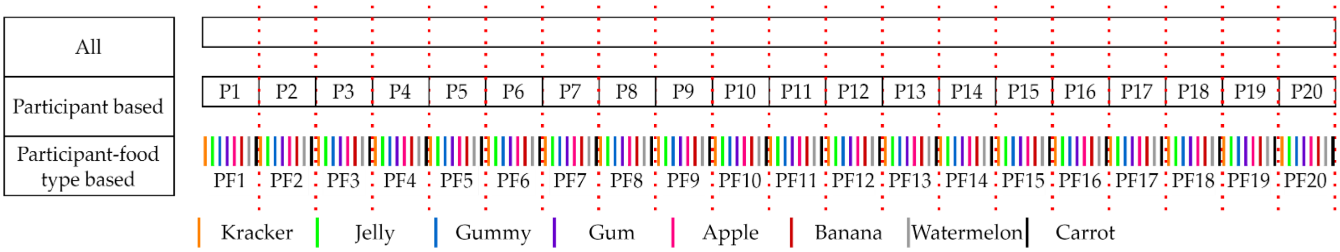

Fig. 5. Overview of the chewing cycle for the whole data of 20 participants.

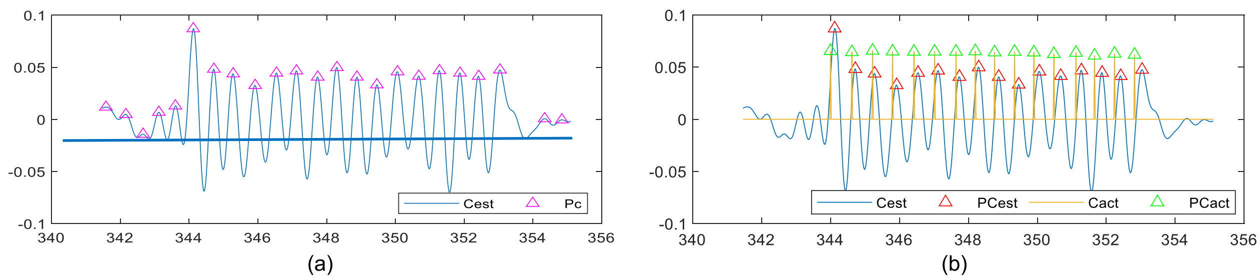

Fig. 6. Detection of peak (a) without and (b) with implementation of prominence and width of the peak.

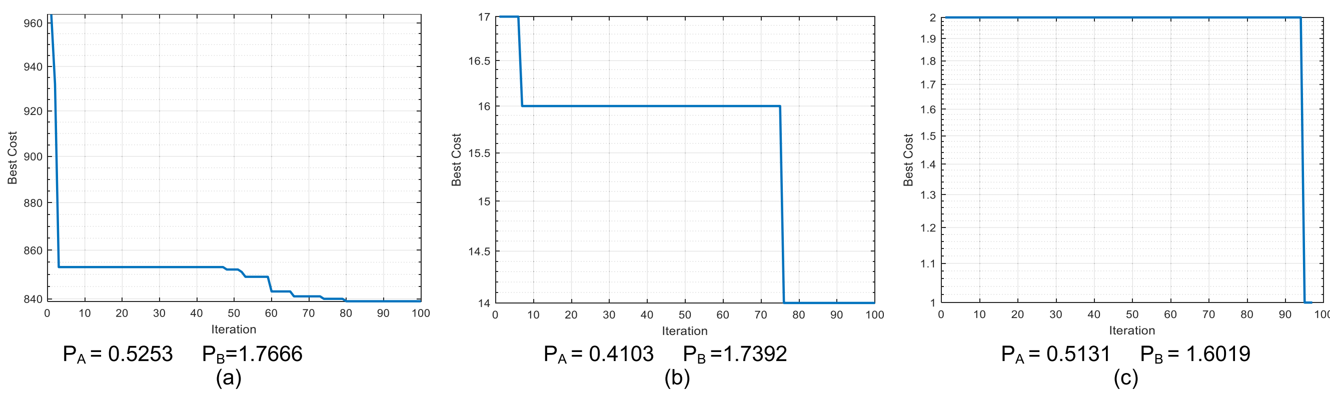

Fig. 7. PSO iteration for chewing cycle of (a) all, (b) participant-based (Participant 13), and (c) participant-food type-based (Participant 13—food type jelly).

given by (5). Here, M represents the total number of chewing episodes, and n denotes the specific chewing episodes for each participant

$$|\%\text{Error}| = \left|\frac{C_{\text{Act}}(n) - C_{\text{Est}}(n)}{C_{\text{Act}}(n)}\right| \times 100 \tag{4}$$

$$|\%\text{Mean Error}| = \frac{1}{M}\sum_{n=1}^{M}\left|\frac{C_{\text{Act}}(n) - C_{\text{Est}}(n)}{C_{\text{Act}}(n)}\right| \times 100. \tag{5}$$

IV. Results, Analysis, and Discussion

For chew count estimation, results were presented as means to analyze the performance of the proposed method. The metrics include the estimated chew count, MAE, average MAE, and PSO computational time.

Chew count was determined by counting peaks in the proximity signal. The PSO algorithm was used to identify the optimal prominence (minimum) and width (maximum) multipliers for accurate chew count estimation. The adaptation of PSO for peak detection is illustrated in Fig. 6. PSO iteration parameters, which search for the optimal solution by minimizing the total absolute error across all chewing cycles, are shown in Fig. 7. Example for participant based and participant food type based of participant 13 with jelly (food type) are depicted in (b) and (c), respectively. The reduction in absolute error from the first to the 100th iteration is illustrated for the three chewing cycle methods: all episodes, participant-based, and participant-food type based, with reductions of 125 (962–837), 3 (17–14), and 1 (2–1), respectively.

The PSO completion times for different methods are provided in Table I. The time taken for the PF method was 400.61 s per participant, for the P method was 469.63 s, and for the A method was 36 621.44 s. Estimations for 20 participants are 8012.2 s for PF, 9392.6 s for P, and 36 621.44 s for A. Thus, PF is faster overall compared to P and A.

Data collected from 720 chewing episodes (36 per participant) are detailed in Table II. The study recorded 30 097 actual chew counts, with 30 136 estimated by method A, 30 115 by method P, and 30 059 by method PF. Fig. 8 plots the estimated total chew counts against the actual counts for all methods.

TABLE I
EXAMPLE OF TIME TAKEN FOR PSO TO FIND THE PARAMETERS

Chewing cycle	A	P_{13}	P_{13}								
			PF_1	PF_2	PF3	PF_4	PF_5	PF_6	PF_7	PF_8	PF_{13t}
Time (s)	36621.44	469.63	46.06	44.24	50.36	33.58	44.08	66.00	44.89	71.40	400.61

TABLE II
DETAILS OF THE CHEW COUNT ESTIMATION

Participants	P_{Cact} (count)	P_{cest} (count)			Mean absolute error (%)			Difference of MAE (%)		
		A	P	PF	A	P	PF	A-P	A-PF	P-PF
1	1705	1677	1693	1707	3.48	2.97	1.01	0.51	2.47	1.96
2	1142	1139	1155	1143	4.75	5.04	1.43	-0.30	3.32	3.62
3	1106	1102	1105	1107	7.45	5.69	2.19	1.76	5.26	3.50
4	1710	1689	1703	1705	2.32	2.00	0.55	0.32	1.77	1.45
5	1153	1172	1155	1157	4.75	3.30	1.32	1.45	3.43	1.97
6	1772	1762	1784	1768	2.57	2.69	0.92	-0.12	1.65	1.77
7	1809	1790	1806	1803	2.38	1.53	0.56	0.85	1.82	0.97
8	1311	1331	1312	1319	6.19	5.47	1.71	0.71	4.47	3.76
9	1147	1182	1155	1158	6.72	5.33	2.57	1.39	4.15	2.76
10	1777	1758	1778	1776	1.49	1.33	0.47	0.16	1.02	0.86
11	1277	1305	1270	1276	5.57	3.48	1.64	2.09	3.93	1.84
12	1246	1263	1238	1208	6.48	5.29	2.13	1.20	4.36	3.16
13	1855	1850	1859	1857	1.46	1.20	0.34	0.26	1.12	0.86
14	1767	1760	1771	1768	2.05	1.62	0.97	0.44	1.09	0.65
15	1830	1815	1836	1834	3.22	1.99	0.53	1.23	2.69	1.46
16	1879	1859	1877	1879	2.14	1.74	0.51	0.41	1.63	1.23
17	1814	1797	1810	1811	2.66	1.92	0.70	0.74	1.96	1.22
18	1271	1299	1281	1272	6.57	6.11	1.73	0.47	4.84	4.38
19	1228	1247	1227	1222	5.63	4.87	2.11	0.76	3.52	2.76
20	1298	1339	1300	1289	7.36	5.59	1.65	1.77	5.71	3.94
Total	30097	30136	30115	30059						
Mean					4.26	3.46	1.25	0.8	3.01	2.21
Std					2.09	1.77	0.69			

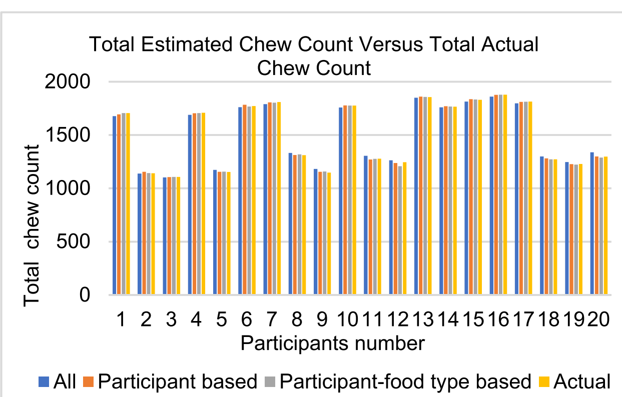

Fig. 8. Total chew count estimation versus total actual chew count plot.

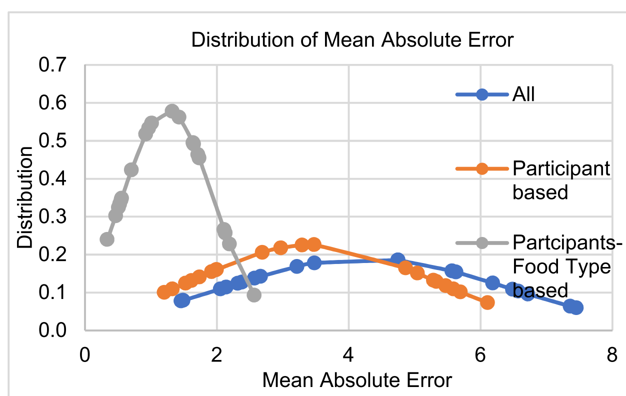

Fig. 9. Distribution of MAE.

The MAE ranged from 1.46% to 7.45% for all chewing cycle methods, with an average of 4.26%. For the P method, the MAE ranged from 1.20% to 5.69%, with an average of 3.46%. The PF method had an MAE range of 0.34%–2.19%. The best MAE was achieved by Participant 13, while the worst was by Participant 3. MAE

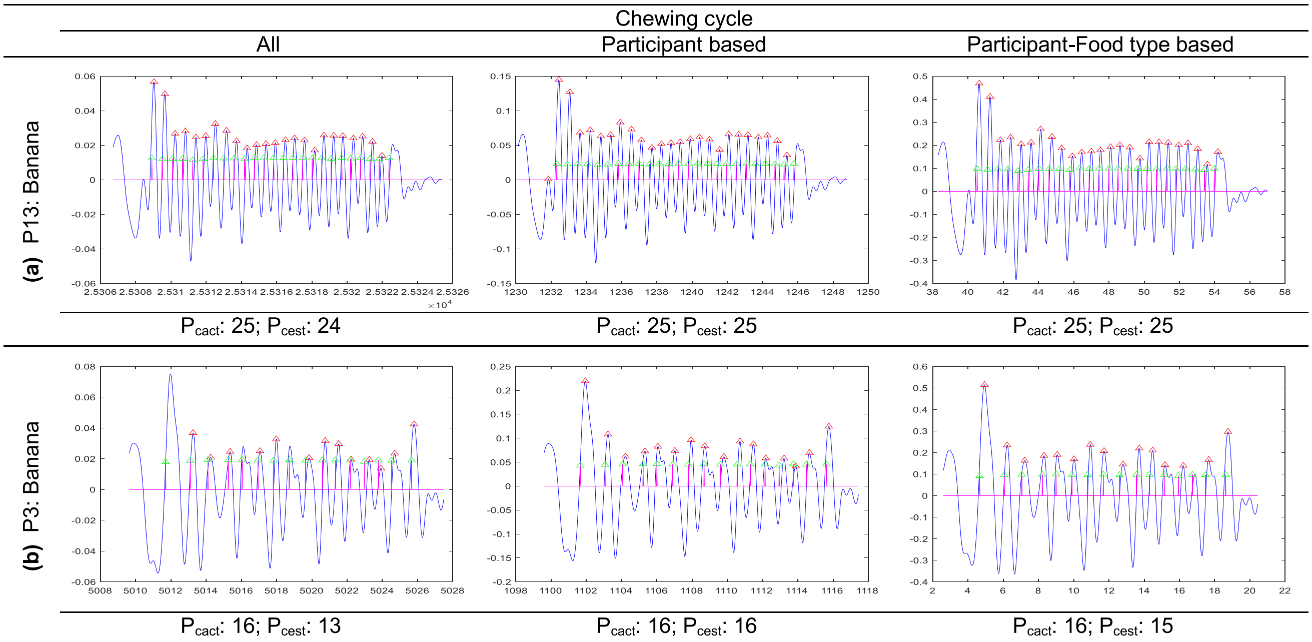

Fig. 10. Example of PSO-peak detection implementation taken from the first chewing episode of the banana (food type). (a) Based on all methods taken from the participants that contribute to the best MAE (Participant 13) and (b) based on all methods taken from the participants that contribute to the worst MAE (Participant 3).

distributions are shown in Fig. 9, with all methods exhibiting a symmetrical shape with a single peak.

The examples of PSO-peak detection implementation for the best (Participant 13) and worst (Participant 3) MAE are provided for the first chewing episode with banana. Fig. 10(a) and (b) illustrates improvements in chew count estimation. For instance, Fig. 10(a) shows that P and PF methods estimate 25 chews, compared to 24 by A. In Fig. 10(b), P and PF methods estimate 16 and 15 chews, respectively, while A estimates 13 chews.

Participant 13 achieved the smallest MAE across all three methods, while Participant 3 had the largest MAE. The MAE for method A was reduced from 4.26% to 3.46% (a 0.80% improvement) using the P method and from 4.26% to 2.21% (a 3.01% improvement) using the PF method. The P method, in turn, was improved from 3.46% to 1.25% (a 2.21% improvement) by the PF method. The PF method showed the greatest improvement over method A, with a 3.01% reduction, followed by the P method with a 2.21% reduction. The difference between the P and PF methods was 0.80%. Overall, the PF method consistently provided the highest improvement across all participants.

The MAE distributions are characterized by symmetrical shapes with a single peak. The chewing cycle method A has a peak at 4.46% with an average of 4.26%. The participant-based method has a peak at 3.48% with an average of 3.46%, while the participant-food type-based method has a peak at 1.32% with an average of 1.25%. The PF method's narrower shape indicates that the values are more concentrated around the mean compared to the A and P methods.

In addition to reducing MAE, the proposed method reduces computational time. The total times for the PF, P, and A methods are 400.6, 469.6, and 36 621.4 s, respectively.

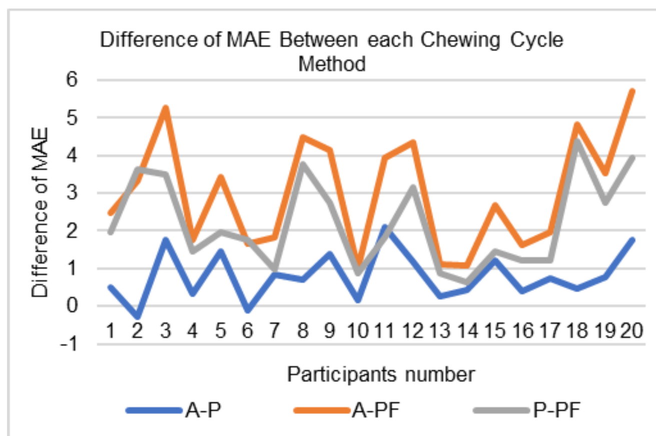

Fig. 11. Difference of MAE in comparison to other methods.

For 20 participants, the estimated completion times are 8012.2 s for PF and 9392.6 s for P. The total completion time for method A is significantly longer at 36 621.4 s. The difference in computational time between methods A and P is 27 229.4 s (74.35%), between A and PF is 28 609.2 s (78.12%), and between P and PF is 1379.8 s (14.69%). Thus, the PF method substantially reduces computational time compared to methods A and P, with P and PF methods differing by only 14.69%.

The differences between methods illustrate the MAE improvements or changes. The P method improved method A by the largest margin of 2.09%, with Participant 11 contributing the best result. For method A compared to PF, the MAE reduction ranged from 1.02% (Participant 10) to 5.71% (Participant 2). The P method compared to PF showed improvements ranging from 0.65% (Participant 14)

TABLE III
SUMMARY OF THE CHEW COUNT METHODS USED IN THE LITERATURE

Reference	Chewing signal data	Methods in estimating the chew count	Feature extracted	Limitation to the peak	Participants Number	Mean absolute error
Proposed	Proximity sensor-Temporalis muscle detection	PSO- peak detection algorithm-Participant-Food type-based	Number of peaks	Minimum peak prominence Maximum peak width	20	1.25%
Proposed	Proximity sensor-Temporalis muscle detection	PSO- peak detection algorithm-Participants based	Number of peaks	Minimum peak prominence Maximum peak width	20	3.46%
[20]	Proximity sensor-Temporalis muscle detection	PSO- peak detection algorithm-All	Number of peaks	Minimum peak prominence Maximum peak width	20	4.26%
[22]	Proximity sensor-Temporalis muscle detection	Peak detection algorithm	Number of peaks	Minimum peak prominence (trial & error)	1	2.69%
[12]	Piezoelectric-lower jaw movement	Peak detection algorithm	Number of peaks	n/a	5	8.09 ± 7.16%
[13]	Piezoelectric-lower jaw movement	Histogram-peak detection algorithm	Number of peaks	The peak must exceed a threshold value (obtained using a histogram)	30	10.4% ± 7.0%
[14]	Piezoelectric-lower jaw movement	Multiple regression model	Number of peaks Valleys Zero crossings Duration	n/a	30	9.66%
[15]	Piezoelectric temporalis muscle detection	Multivariate regression model	Number of peaks Zero crossings Duration	n/a	10	3.43%
[19]	Triaxial accelerometer on the temporalis	MFC	The peak of the z-axis of the accelerometer	n/a	4	12.2%
[7]	Video recording	Deep learning and affine optical flow	Number of peaks	n/a	28	Mean accuracy 88.9% ±7.4%
[16]	Video recording	Image processing of chewing videos No.	Number of peaks	Minimum peak height	100	5.42% ± 4.61 (slow) 7.47% ± 6.85 (normal) 9.84% ± 9.55 (fast)
[17]	Optical distance sensor-Earphone type	n/a	Peak to Peak	n/a	6	Precision ≥0.958

to 4.38% (Participant 18). Fig. 11 illustrates the MAE differences between methods for each participant, showing that the PF method generally provided the largest improvement.

For a comprehensive comparison of chew count estimation methods, we review and compare those presented in previous literature. To the best of our knowledge, ten articles have discussed various chew count methods. Of these, eight employed sensors, such as piezoelectric sensors, accelerometers, optimal distance sensors, and PSs, typically placed on the jaw or temporalis muscle to detect chewing. Two studies utilized video recordings, which were processed to extract the chewing signal.

All methods reviewed for chew count estimation rely on peak counting. Four articles applied specific limitations for peak detection, including threshold values [13], minimum peak height [16], prominence of the peak obtained through trial and error [22], and argument implementation of minimum peak prominence, and a combination of minimum peak prominence and maximum peak width using PSO [20]. The most common performance measurement for chew count is the MAE. The MAE values for different sensors are as follows: piezoelectric sensors 8.09 ± 7.16% [12], 10.4% ± 7.0% [13], 9.66% [14], 3.43% [15], the accelerometer 12.2%, and the PSs 2.69% [22], 4.26% [20].

A summary of the chew count methods proposed in the literature, compared to the method presented in this article, is provided in Table III.

V. CONCLUSION

This article introduces new chewing cycle methods to optimize the PSO approach for chew count estimation using minimum peak prominence and maximum peak width in a peak detection algorithm. The study utilizes PS data, capturing chewing signals from temporalis muscle movements. These signals were preprocessed with z-score normalization, a bandpass filter of 0.3–2.2 Hz, a 3-s window size, and a peak detection system constrained by peak prominence and width.

Chewing patterns vary between individuals, influenced by factors, such as facial structure, masticatory muscle properties, and food type. To address this variability, this study proposes two chewing cycles: one based on individual participants and the other on a combination of participants and food types. These cycles aim to enhance chew count estimation by accounting for participant and food type diversity.

The PSO-peak detection algorithm provides different parameter combinations depending on the chewing cycle: A cycle is one combination of two parameters (P_A and P_B). P cycle is 20 combinations of two parameters. PF cycle is 160 combinations of two parameters.

Results indicate that the PF method yields the lowest MAE at 1.25%, followed by the P method at 3.46%, and the A method at 4.26%. The MAE distribution for the PF method is narrower compared to the A and P methods, suggesting higher probability and consistency around the mean. Additionally, the PF method requires the shortest computation time (8012.2 s), followed by the P method (9392.0 s), while the A method demands the longest time (36 621.4 s).

Future research will explore inter- and intrasubject variabilities, assessing the suitability of subject groups for quantitative evaluation. Additionally, the robustness of the proposed method will be tested for chew count estimation using data collected during physical activities.

Acknowledgment

Nur Asmiza Selamat is with the Department of Electric, Electronic and Systems Engineering, Universiti Kebangsaan Malaysia, Bangi, Selangor 43600, Malaysia, and also with the Fakulti Teknologi dan Kejuruteraan Elektrik, Universiti Teknikal Malaysia Melaka, Durian Tunggal, Melaka 76100, Malaysia (e-mail: nurasmiza@utem.edu.my).

Sawal Hamid Md Ali is with the Department of Electric, Electronic and Systems Engineering, Universiti Kebangsaan Malaysia, Bangi, Selangor 43600, Malaysia (e-mail: sawal@ukm.edu.my).

Ahmad Ghadafi Ismail is with the Institute of Microengineering and Nanoelectronics (IMEN), Universiti Kebangsaan Malaysia, Bangi, Selangor 43600, Malaysia (e-mail: ghad@ukm.edu.my).

Siti Anom Ahmad is with the Faculty of Engineering, Universiti Putra Malaysia (UPM), Serdang, Selangor 43400, Malaysia (e-mail: sanom@upm.edu.my).

Khairun Nisa' Minhad is with the Department of Electrical and Electronic Engineering, Xiamen University Malaysia, Bandar Sunsuria, Sepang, Selangor 43900, Malaysia (e-mail: khairunnisa.minhad@xmu.edu.my).

References

[1] L. Wang et al., "Enhancing nutrition care through real-time, sensor-based capture of eating occasions: A scoping review," *Frontiers Nutrition*, vol. 9, pp. 1–14, May 2022, doi: 10.3389/fnut.2022.852984.

[2] Q. Huang, W. Wang, and Q. Zhang, "Your glasses know your diet: Dietary monitoring using electromyography sensors," *IEEE Internet Things J.*, vol. 4, no. 3, pp. 705–712, Jun. 2017, doi: 10.1109/JIOT.2017.2656151.

[3] W. Bangamuarachchi, A. Chamantha, L. Meegahapola, S. Ruiz-Correa, I. Perera, and D. Gatica-Perez, "Sensing eating events in context: A smartphone-only approach," *IEEE Access*, vol. 10, pp. 61249–61264, 2022, doi: 10.1109/ACCESS.2022.3179702.

[4] X. Yang et al., "Statistical models for meal-level estimation of mass and energy intake using features derived from video observation and a chewing sensor," *Sci. Rep.*, vol. 9, no. 1, pp. 1–10, Jan. 2019, doi: 10.1038/s41598-018-37161-x.

[5] A. Bedri, D. Li, R. Khurana, K. Bhuwalka, and M. Goel, "FitByte: Automatic diet monitoring in unconstrained situations using multimodal sensing on eyeglasses," in *Proc. CHI Conf. Hum. Factors Comput. Syst.*, Apr. 2020, pp. 1–12, doi: 10.1145/3313831.3376869.

[6] B. M. Bell et al., "Automatic, wearable-based, in-field eating detection approaches for public health research: A scoping review," *NPJ Digit. Med.*, vol. 3, no. 1, p. 14, Mar. 2020, doi: 10.1038/s41746-020-0246-2.

[7] D. Hossain, T. Ghosh, and E. Sazonov, "Automatic count of bites and chews from videos of eating episodes," *IEEE Access*, vol. 8, pp. 101934–101945, 2020, doi: 10.1109/ACCESS.2020.2998716.

[8] S. Wang et al., "Inferring food types through sensing and characterizing mastication dynamics," *Smart Health*, vol. 20, Apr. 2021, Art. no. 100191.

[9] N. A. Selamat and S. H. M. Ali, "Automatic food intake monitoring based on chewing activity: A survey," *IEEE Access*, vol. 8, pp. 48846–48869, 2020, doi: 10.1109/ACCESS.2020.2978260.

[10] J. M. Fontana et al., "Energy intake estimation from counts of chews and swallows," *Appetite*, vol. 85, pp. 14–21, Feb. 2015, doi: 10.1016/j.appet.2014.11.003.

[11] G. Hussain, B. A. S. Al-Rimy, S. Hussain, A. M. Albarrak, S. N. Qasem, and Z. Ali, "Smart piezoelectric-based wearable system for calorie intake estimation using machine learning," *Appl. Sci.*, vol. 12, no. 12, p. 6135, Jun. 2022, doi: 10.3390/app12126135.

[12] M. Farooq and E. Sazonov, "Comparative testing of piezoelectric and printed strain sensors in characterization of chewing," in *Proc. 37th Annu. Int. Conf. IEEE Eng. Med. Biol. Soc. (EMBC)*, Aug. 2015, pp. 7538–7541, doi: 10.1109/EMBC.2015.7320136.

[13] M. Farooq and E. Sazonov, "Automatic measurement of chew count and chewing rate during food intake," *Electronics*, vol. 5, no. 4, p. 62, Sep. 2016, doi: 10.3390/electronics5040062.

[14] M. Farooq and E. Sazonov, "Linear regression models for chew count estimation from piezoelectric sensor signals," in *Proc. 10th Int. Conf. Sens. Technol. Linear*, 2016, p. 5, doi: 10.1109/BIBM.2007.18.

[15] M. Farooq and E. Sazonov, "Segmentation and characterization of chewing bouts by monitoring temporalis muscle using smart glasses with piezoelectric sensor," *IEEE J. Biomed. Health Informat.*, vol. 21, no. 6, pp. 1495–1503, Nov. 2017, doi: 10.1109/JBHI.2016.2640142.

[16] S. Alshboul and M. Fraiwan, "Determination of chewing count from video recordings using discrete wavelet decomposition and low pass filtration," *Sensors*, vol. 21, no. 20, p. 6806, Oct. 2021, doi: 10.3390/s21206806.

[17] K. Taniguchi, H. Kondo, T. Tanaka, and A. Nishikawa, "Earable RCC: Development of an earphone-type reliable chewing-count measurement device," *J. Healthcare Eng.*, vol. 2018, pp. 1–8, Jan. 2018, doi: 10.1155/2018/6161525.

[18] S. Zhang et al., "NeckSense: A multi-sensor necklace for detecting eating activities in free-living conditions," *Proc. ACM Interact., Mobile, Wearable Ubiquitous Technol.*, vol. 4, no. 2, pp. 1–26, Jun. 2020, doi: 10.1145/3397313.

[19] S. Wang et al., "Eating detection and chews counting through sensing mastication muscle contraction," *Smart Health*, vols. 9–10, pp. 179–191, Dec. 2018, doi: 10.1016/j.smhl.2018.07.004.

[20] N. A. Selamat, S. H. M. Ali, K. N. B. Minhad, S. A. Ahmad, and J. Sampe, "A novel peak detection algorithm using particle swarm optimization for chew count estimation of a contactless chewing detection," *IEEE Trans. Instrum. Meas.*, vol. 71, pp. 1–12, 2022, doi: 10.1109/TIM.2022.3220281.

[21] N. A. Selamat and S. H. M. Ali, "A novel approach of chewing detection based on temporalis muscle movement using proximity sensor for diet monitoring," in *Proc. IEEE-EMBS Conf. Biomed. Eng. Sci. (IECBES)*, Mar. 2021, pp. 12–17.

[22] N. A. Selamat and S. H. Ali, "Analysis of chewing signals based on chewing detection using proximity sensor for diet," in *Proc. ICPR Workshops*, vol. 12665, 2021, pp. 599–616, doi: 10.1007/978-3-030-68821-9.

Nur Asmiza Selamat (Member, IEEE) received the bachelor's degree in electrical engineering and the M.Eng. degree in mechatronics and automatic control engineering from Universiti Teknologi Malaysia (UTM), Skudai, Johor, Malaysia, in 2009 and 2013, respectively. She is currently pursuing the Ph.D. degree with Universiti Kebangsaan Malaysia (UKM), Bangi, Selangor, Malaysia.

From 2009 to 2010, she was an Electrical Engineer at Tenaga Nasional Berhad (TNB), Malaysia. From 2010 to 2011, she is a Tutor at Universiti Teknikal Malaysia Melaka (UTeM), Durian Tunggal, Melaka, Malaysia. Since 2013, she has been a Lecturer at the Fakulti Teknologi dan Kejuruteraan Elektrik, UTeM.

Sawal Hamid Md Ali (Senior Member, IEEE) received the bachelor's degree in electronic and computer engineering from Universiti Putra Malaysia, Serdang, Selangor, Malaysia, in 1998, and the master's degree in microelectronic system design and the Ph.D. degree in electrical and electronics from the University of Southampton, Southampton, U.K., in 2004 and 2010, respectively.

He is currently the Deputy Director of the Centre for Innovation and Technology Transfer. He is also a Professor with the Department of Electrical, Electronics and System Engineering, Universiti Kebangsaan Malaysia, Bangi, Selangor, Malaysia.

Dr. Md Ali is a member of the Institute of Electrical and Electronics Engineers (IEEE) Circuit and Systems Society. He was a recipient of the ASEAN-US Science and Technology Fellowship, from 2016 to 2017.

Ahmad Ghadafi Ismail (Member, IEEE) received the M.Sc. degree from the University of Southern California, Los Angeles, CA, USA, in 2002, and the Ph.D. degree from Dalhouse University, Halifax, NS, Canada, in 2011.

He is a Senior Lecturer at Universiti Kebangsaan Malaysia (UKM), Bangi, Selangor, Malaysia.

Siti Anom Ahmad (Senior Member, IEEE) received the B.Eng. degree in electronic computer from Universiti Putra Malaysia (UPM), Serdang, Selangor, Malaysia, in 1999, and the M.Sc. degree in microelectronics system design and the Ph.D. degree in electrical and electronics from the University of Southampton, Southampton, U.K., in 2004 and 2009, respectively.

She is also a Professor with the Faculty of Engineering, UPM. Her research interests include biomedical engineering, geotechnology, and intelligent control systems.

Dr. Ahmad is a Professional Engineer of the Board of Engineers Malaysia, a Chartered Engineer of the Institute of Engineering and Technology (IET), U.K., and a member of the Institute of Engineers Malaysia (IEM).

Khairun Nisa' Minhad (Member, IEEE) received the B.Eng. (Hons.) degree in microelectronics from Universiti Teknologi Malaysia, Malaysia, in 1998, and the M.Sc. degree in microelectronics and the Ph.D. degree in electrical, electronic, and systems engineering from Universiti Kebangsaan Malaysia, Bangi, Selangor, Malaysia, in 2013 and 2019, respectively.

She worked as a Design Engineer at Altera Corporation Malaysia Sdn. Bhd. (currently known as Intel Malaysia), Penang, Malaysia, from 1998 to 2011. She joined Xiamen University Malaysia, Sepang, Malaysia, in 2019, as an Assistant Professor at the Department of Electrical and Electronic Engineering. Her research interests are VLSI design (analog/digital IC design and IC mask design) and biomedical engineering (biomedical signal processing and analysis, biomedical application IC, and wearable sensors).